Studying Pulse-forming Networks with Help of Computer Simulation

Oleksandr Pliushch[a], Yurii Kravchenko[a] and Anatolii Rybydajlo[b]

[a] *Taras Shevchenko National University of Kyiv, 60 Volodymyrska Street, Kyiv, 01601, Ukraine*
[b] *Center for Military and Strategic Studies of the National Defence University of Ukraine named after Ivan Cherniakhovskyi, 28 Povitroflotskyi Ave, Kyiv, 03049,Ukraine*

Abstract

Processes in pulse-forming networks are studied. It is stressed that selecting such a pulse-forming network that provides the desired pulse form at the output is the main problem in a pulse modulator design. This mathematical problem in network synthesis usually involves analytical methods that are very difficult and time consuming for obtaining time-domain response of a pulse-forming network. The paper proposes investigating transient performances in artificial transmission lines with help of computer simulation in Matlab environment. A number of computer models are created, and they are tested for different scenarios of pulse-forming networks operation. Obtained results clearly indicate validity of the models and their usefulness for studying time-domain responses of pulse-forming networks of different types. Designed models can be used in conducting promising research in the respective field or testing efficiency of already existing installations.

Keywords [1]

Pulse-forming networks, artificial transmission lines, time-domain response, computer simulation, Matlab

1. Introduction

This paper studies processes in artificial transmission lines using computer simulation in Matlab environment. Those lines, also known as pulse-forming networks, are an important element of a pulse modulator that determines, to a large extent, parameters of a transmitter or generator, in which the modulator is deployed [1, 2, 3, 4, 15] . Mentioned power devices are widely used as a component of a pulsed radar or as a radio element in theoretical physics installations [4, 7, 14].

The main problem that presents itself in a pulse modulator designing is that of selecting such a pulse-forming network that secures the required pulse form at the output [5, 6, 14]. The term “pulse form” means the shape derived when the pulse amplitude is plotted as a function of time. Particular details of interest of a pulse shape are known as “leading edge,” the “top,” and the “trailing edge” of the pulse [4, 7]. A current pulse of ideal rectangular form is required for a power amplifier, such as magnetron or klystron, to avoid output frequency or phase deviations. In theory, this rectangular pulse form can be obtained using “natural” transmission line, but this is not feasible in real installations for a number of reasons; as a result, artificial transmission lines are used.

The development of pulse-forming networks that simulate natural transmission lines is a mathematical problem in network synthesis [7]. As may be anticipated, no network having a finite number of elements can exactly simulate a transmission line which in reality has distributed rather than lumped parameters. As the number of elements for a given network type is increased, the degree of simulation will improve. It may happen, however, that the network pulse is a good approximation to the rectangular pulse during only a portion of the pulse interval. For example, the network pulse may exhibit overshoots and excessive oscillations, especially near the beginning and the end of the pulse. These possibilities must be kept in mind, and the properties of networks derived by formal mathematical methods must be investigated with care to determine how closely the networks approximate transmission lines. Artificial transmission lines or pulse forming networks can be

Information Technology and Implementation (IT&I-2021), December 01–03, 2021, Kyiv, Ukraine
EMAIL: opliusch@yahoo.com (A. 1); kr34@ukr.net (A. 2); rybydajlo307@ukr.net (A. 3)
ORCID: 0000-0001-5310-0660 (A. 1); 0000-0002-0281-4396 (A. 2); 0000-0002-6156-469X (A. 3)
© 2021 Copyright for this paper by its authors.
Use permitted under Creative Commons License Attribution 4.0 International (CC BY 4.0).
CEUR Workshop Proceedings (CEUR-WS.org)

CEUR-WS.org/Vol-3179/Short_11.pdf

homogenous, with the same values of capacitors and inductors in each stage, and heterogeneous, with those values being different to a great extent. Studying performance of a homogenous artificial line using analytical methods is difficult and to obtain a pulse form in time domain requires solving complex polynomials of a very high order [7, 8, 9]. Heterogeneous pulse forming networks are even harder to analyze although they are used more often due to their better characteristics.

Computer simulation becomes more and more powerful tool in studying different processes and installations [11, 12, 13]. This paper proposes investigating artificial transmission lines with help of computer simulation in Matlab environment. The approach provides reasonable accuracy as well as simplicity and is illustrative and descriptive.

2. General description of a pulse modulator performance

2.1. Functional diagram

In many applications that include, naming just a few, radars or theoretical physics installations energy on radio frequencies is emitted in short pulses. Time durations of those pulses can be somewhere between 2 to 30 microseconds or even more [7]. This type of a switched oscillator or transmitter needs a special modulator. The modulator creates impulses of high voltage turning the microwave device on/off. The hydrogen thyratron modulator is still most widely used in such a modulator [1]. Pulse-forming network (PFN), as is shown in figure 1 (borrowed from [1]), is the main component of such an installation. This PFN or artificial transmission line is charged up slowly to a high value of voltage during the first stage of operation. Then in the second stage, the network is discharged rapidly through a pulse transformer by the switching device such as thyratron to develop an output pulse; the shape and duration of the pulse are determined by the electrical characteristics of the pulse-forming network and of the pulse transformer. A short section of artificial transmission line or PFN is used to store energy that it accumulates during the charge stage. In the process, this PFN is charged on the double voltage of the high voltage power supply with help of the magnetic field of the charging coil. Another role of this coil is to limit the charging current. The charging diode prevents the PFN from discharging itself when the maximum voltage is reached.

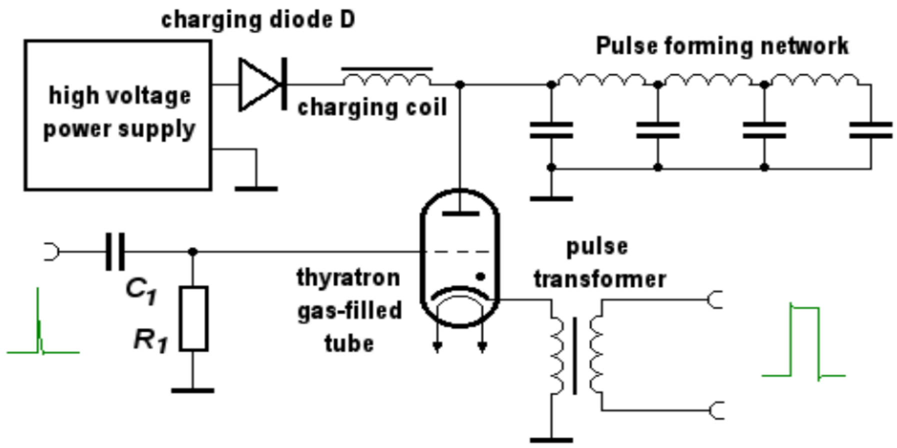

Figure 1: Thyratron Modulator

The function of thyratron is to act as an electronic switch which requires a positive trigger of only around 150 volts [1]. The thyratron requires a sharp leading edge for a trigger pulse and depends on a sudden drop in anode voltage (controlled by the pulse-forming network) to terminate the pulse and cut off the tube. The *R*-*C* element acts as a DC- shield and protect the grid of the thyratron. This trigger pulse initiates the ionization of the complete thyratron by the charging voltage. This ionization allows conduction from the charged pulse-forming network through pulse transformer. The output pulse is then applied to an oscillating device, such as a magnetron.

2.2. The Charge Path

The charge path includes the primary of the pulse transformer, the DC power supply, and the charging impedance. The thyratron (as the modulator switching device) is an open circuit in the time between the trigger pulses. Therefore, it is shown as an open switch in figure 2 (borrowed from [1]).

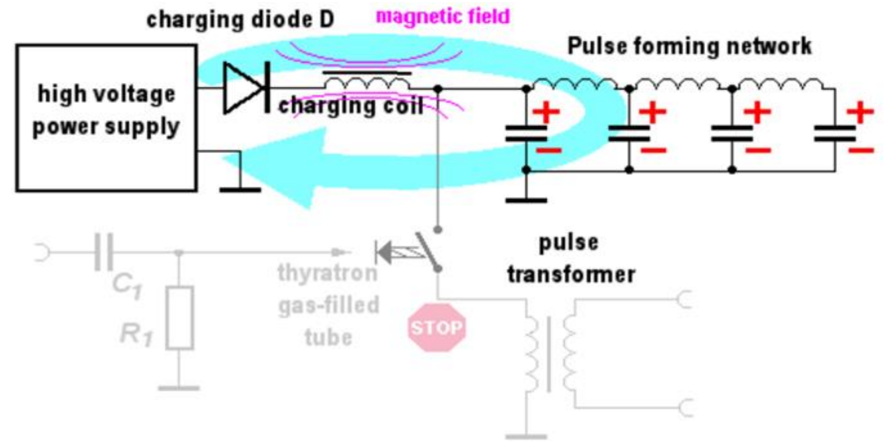

Figure 2: Charging currents path

Once the power supply is switched on, the current flows through the charging diode and the charging impedance (coil) and charges the condensers of the pulse forming network. The coils of the PFN are not yet functional. However, the induction of the charging impedance offers a great inductive resistance to the current and builds up a strong magnetic field. The charging of the condensers follows an exponential pattern. The self- induction of the charging impedance overlaps for this.

2.3. The Discharge Path

When a positive trigger pulse is applied to the grid of the thyratron, the tube ionizes causing the pulse-forming network to discharge through the thyratron and the primary of the pulse transformer, as is shown in figure 3 (borrowed from [1]).

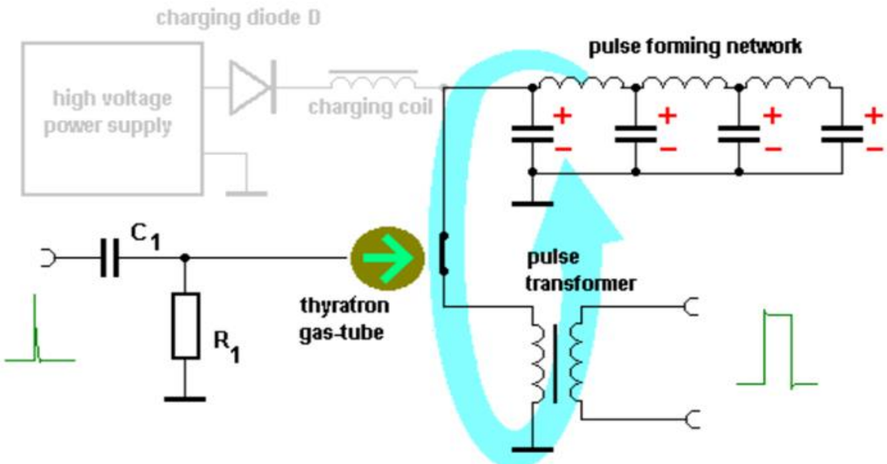

Figure 3: Discharging currents path

The fired thyratron grounds the pulse line at the charging coil and the charging diode effectively. Therefore, a current flows for the duration of pulse width through the pulse transformer primary coil to ground and from ground through the thyratron, which is now conducting to the other side of the pulse forming network. The high voltage pulse for the transmitting tube can be taken on the secondary coil of the pulse transformer. Exactly for this time an oscillating device generates on the transmit frequency. Because of the inductive properties of the PFN, the positive discharge voltage has a tendency to swing negative. If the oscillator and pulse transformer circuit impedance is properly matched to the line impedance, the voltage pulse that appears across the transformer primary equals one-half of the voltage to which the line was initially charged. The most important observation from the processes above is that the switch only initiates the discharge of the energy stored in the PFN. At the same time, the shape and duration of the pulse are determined by the passive elements of the PFN. The switch has no control over the pulse shape other than to initiate it. The pulse ends when the PFN has discharged sufficiently. A disadvantage of this action is that the trailing edge of the pulse is usually not sharp since it depends on the discharge characteristics of the PFN.

3. Synthesis of mathematical models of pulse-forming networks
3.1. Mathematical model of Type B pulse-forming network

There are a number of pulse-forming networks, and they are differentiated using letters B, C, D, E, and F [4, 7]. For the purpose of this research, only two of them are chosen; they are those PFN that are most widely used and, at the same time, are most opposite in their structure.

First, let us consider type B network, which is presented in figure 4. Here, the pulse-forming network is depicted for the case of five stages although there can be more elements. If values of all capacitors and inductors in figure 4 are the same, then the pulse-forming network is considered homogeneous; if those values are different for different stages, then the artificial transmission line is referred to as heterogeneous. In this paper both of them are considered.

During the discharge process, the line is loaded with the resistor R_L, also shown in figure 4.

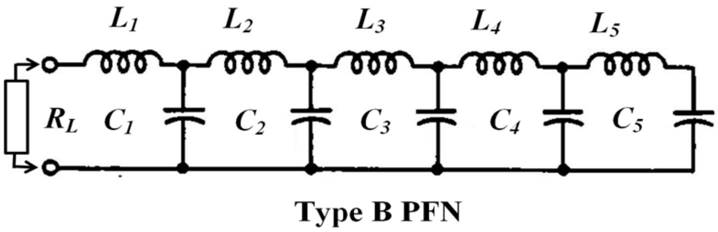

Figure 4: Type B pulse-forming network

Now, let us proceed to synthesizing a mathematical model for the pulse-forming network in figure 4. Circuit diagraph in this figure includes three typical electrical elements: they are R, L, and C. Relationships between voltages and currents, which are referred to as constitutive relations, for these radioelements are known to be as follows [6, 11]:

$$v(t) = Ri(t), \tag{1}$$

$$i(t) = C\frac{dv(t)}{dt} \text{ or } v(t) - v(0) = \frac{1}{C}\int_0^t i(\tau)d\tau, \tag{2}$$

$$v(t) = L\frac{di(t)}{dt} \text{ or } i(t) - i(0) = \frac{1}{L}\int_0^t v(\tau)d\tau. \tag{3}$$

The constitutive relation for resistor is illustrated by (1), while those for capacitor and inductor elements - by (2) and (3) respectively. Mathematical models of electrical systems that include L, C and R elements can be derived using a systematic two-step process [6, 11]. First, one needs to write the corresponding first-order ordinary differential equations (ODE) for each energy-storage element (capacitor or inductor). The dynamic variables of the ODEs will be either voltage $v_C(t)$ (for a capacitor) or current $i_L(t)$ (for an inductor).

Second, it is necessary to use Kirchhoff's laws to express the unknown voltages and currents in terms of either the dynamic variables associated with the energy-storage elements ($v_C(t)$ or $i_L(t)$) or the sources (input voltage U_{in} or input current I_{in}). Applying Kirchhoff's laws to the first circuit loop in the circuit diagram in figure 4, one can derive following equations:

$$V_{C1} + V_{L1} + V_{RL} = 0, \tag{4}$$

$$I_{L1} + I_{C1} + I_{L2} = 0. \tag{5}$$

The same procedure with respect to the loops beginning from the second and finishing by the last leads to the following results:

$$I_{Ci} + I_{Li} + I_{Li+1} = 0, \tag{6}$$

$$V_{Ci} + V_{Ci-1} + V_{Li} = 0. \tag{7}$$

Substituting constitutive relations (1), (2), and (3) into (4), (5), (6), and (7), the following system of differential equations can be derived:

$$C\frac{dv_{C1}(t)}{dt} = -i_{L1}(t) - i_{L2}(t), \tag{8}$$

$$L\frac{di_{L1}(t)}{dt} = -\,v_{C1}(t) - R_L i_{L1}(t), \tag{9}$$

$$C\frac{dv_{Ci}(t)}{dt} = -i_{Li}(t) - i_{Li+1}(t), \tag{10}$$

$$L\frac{di_{Li}(t)}{dt} = -\,v_{Ci}(t) - v_{Ci-1}(t). \tag{11}$$

Equations (8), (9), (10), and (11) represent the mathematic model of the circuit diagram in figure 4 for continuous time and can be used to study its behavior. However, this approach is characterized by certain difficulties and lacks some clarity in understanding processes. To avoid these problems and analyze a wider range of practical systems and devices, it is proposed to transition from the continuous time to the discrete one and replace the differential equations with difference ones.

The discrete time representation of differential equations by difference ones almost always includes replacing derivatives in (8), (9), (10), and (11) by formulas involving differences. One of the possible approaches, known as forward Euler algorithm, can be presented as:

$$\frac{dx(t)}{dt} = \frac{x(t+\Delta t)-x(t)}{\Delta t}, \tag{12}$$

where Δt is the step size that is assumed fixed.

The circuit diagram of the transmission line in figure 4 has a regular structure. This fact greatly simplifies its computer simulation using cycles in computer programming for both elements and iterations. Applying (12) to (8), (9), (10), and (11), with account of the polarity of currents and voltages, one can derive the following difference equations system:

$$i_{L1}(n+1) = -\frac{\Delta t}{L_1}\, v_{C1}(n) + i_{L1}(n)\left(1 - \frac{R_L \Delta t}{L}\right), \tag{13}$$

$$v_{C1}(n+1) = v_{C1}(n) + i_{L1}(n)\frac{\Delta t}{C_1} - i_{L2}(n)\frac{\Delta t}{C_1}, \tag{14}$$

$$i_{Li}(n+1) = i_{Li}(n) - v_{Ci}(n)\frac{\Delta t}{L} + v_{Ci-1}(n)\frac{\Delta t}{L}, \tag{15}$$

$$v_{Ci}(n+1) = v_{Ci}(n) + i_{Li}(n)\frac{\Delta t}{C_i} - i_{Li+1}(n)\frac{\Delta t}{C_i}, \tag{16}$$

where *i* denotes the number of the loop in the circuit, *n* – iteration number and Δ – the time interval between iterations. Equations (13), (14), (15), and (16) represent a mathematical model of discrete time for the pulse-forming line in figure 4, which is very convenient for computer simulation.

3.2. Mathematical model of Type C pulse-forming network

Another type of pulse-forming network is shown in figure 5 and is known as Type C [4, 7]. It is claimed in the literature that with proper selection of the elements' values, the transient performance of the pulse forming networks in figure 4 and figure 5 is identical. The computer models designed in this paper can be helpful in clarifying those claims. Let us synthesize model for the circuit depicted in figure 5. The approach to deriving the model is the same as above. In the first step, Kirchhoff's laws are applied to the circuit diagram in figure 5, and the following system of equations is obtained:

$$I_{RL} = \sum_{k=i}^{N} I_{Li,} \tag{17}$$

$$V_{Li} = -V_{RL} + U_{Ci}, \tag{18}$$

$$I_{Ci} = -I_{Li}, \tag{19}$$

where *i* is the number of a parallel branch (there are five of them in the figure), *N* is the number of branches.

With account of (1), (2), and (3), the following system of differential equations can be derived in terms of the dynamic variables associated with the energy-storage elements (*L* and *C*):

$$i_{RL}(t) = \sum_{k=i}^{N} i_{Li}(t), \tag{20}$$

$$L_i \frac{di_i(t)}{dt} = v_{Ci}(t) - i_{RL}(t)R_L, \tag{21}$$

$$C_i \frac{dv_{Ci}(t)}{dt} = i_{Li}(t), \tag{22}$$

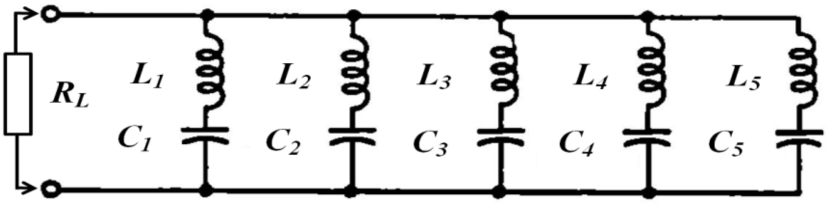

Figure 5: Type C pulse-forming network

Consistently applying (12) to (20), (21) and (22), one can derive the system of the following difference equations:

$$i_{RL}(n) = \sum_{k=i}^{N} i_{Li}(n), \tag{23}$$

$$i_i(n+1) = i_i(n) + \frac{\Delta t}{L_i} v_{Ci}(t) - \frac{\Delta t}{L_i} i_{RL}(t)R_L, \tag{24}$$

$$v_{Ci}(n+1) = v_{Ci}(n) + \tfrac{\Delta t}{C_i} i_{Li}(n). \tag{25}$$

Recurrent formulas (23), (24) and (25) represent the computer model of discrete time for the pulse forming network in figure 5, which is similar to the one constituted by (13), (14), (15), and (16). Those two models can now be used to study pulse-forming networks in figure 4 and figure 5.

4. Computer simulation of Type B network

Let us first perform computer simulation for the homogenous Type B pulse-forming network presented in figure 4. For this purpose, equations (13), (14), (15), and (16) were used to create a program in Matlab environment. Values of capacitors and inductors for homogenous artificial transmission line are calculated according to the formulas

$$L = (TR_L)/(2N), \tag{26}$$

$$C = T/(2NR_L), \tag{27}$$

where T is the required pulse duration, R_L is the load resistor of the line and N is the number of stages in the line.

Let us assume that one would like to obtain a pulse with the duration 10 μs on the load resistor 100 ohms. In this case, for the 5 stage pulse-forming network, values of C and L, respectively are 1.0e-08 F and 1.0e-04 H. Initial charge of the line is 10 V. Figure 6 presents the shape of the discharge pulse for the initial data shown above as a result of the computer simulation in Matlab using the developed model. By inspection, overshoots of the voltage and some unwanted oscillations are clearly visible. Leading edge of the pulse, the top and the trailing edge of the pulse are also indicated. It is necessary to stress that the shape is the same for these conditions, as the one that can be found in the literature [7, 16]. A great deal of effort has been done to improve the shape of the pulse in figure 6 [4, 17, 18]. All of them are directed at using heterogeneous pulse-forming networks in which values of the capacitors and inductors are different. It is known from the literature [4, 7] that the five-section network can produce a trapezoidal pulse with a rise time of about 8 percent if it has parameters shown in table1. Values in this table should be multiplied for capacitors by T/R_L and for inductors by TR_L [4, 7, 19] Just to remind, T is the pulse duration, which is 10 μs, and R_L is the load resistor of the pulse-forming network, which is 100 ohms. Figure 7 illustrates the pulse shape produced by heterogeneous

Type B pulse-forming network with the values of conductors and inductors as stated in Table 1. In the same figure, the curve from figure 6 is added for comparison.

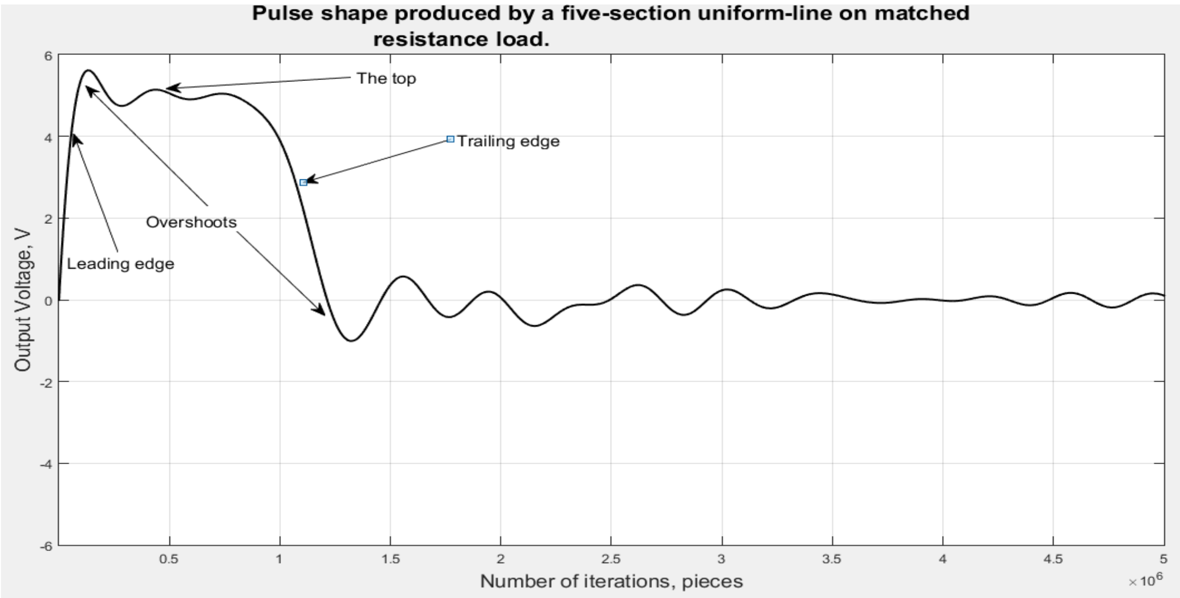

Figure 6: Pulse shape produced by homogeneous Type B pulse-forming network with 5 elements on matched load

Table 1
Values of capacitors and inductors to form a trapezoidal pulse in Type B PFN

Stage number	Capacitor value	Inductance value
1	0.0646	0.0781
2	0.0642	0.0632
3	0.0703	0,0658
4	0,0890	0.0774
5	0.1674	0.1093

As observed from figure 7, non-uniform or heterogeneous pulse forming line with the parameters from table 1 really creates trapezoid pulse shape that demonstrates better performance as compared to the pulse shape in figure 6, which is especially significant for the trailing edge. Still, the main inference is that the model designed in this paper adequately describes performance of the pulse-forming network in different scenarios of operation. In additions, it presents itself as a powerful tool to study different processes in pulse-forming networks that are difficult to study by analytical methods. Parameters in the model may be quickly changed to modify the experiment.

5. Computer simulation of Type C network

Let us now consider performance of the Type C network presented in figure 5 [4, 7, 20]. It is known from several sources that PFNs in figure 4 and figure 5 lead to identical pulses during their discharge. If the developed model can show it, it would be another proof of its validity.

Table 2 includes values of capacitors and conductors for Type C PFN shown in figure 5 that generates trapezoidal pulse. Let us not forget that the values in this table should be multiplied for capacitors by T/R_L and for inductors by TR_L, as is done above. Figure 8 demonstrates pulse shape obtained for heterogeneous Type C pulse-forming network with 5 elements on matched load, which is presented in figure 5. To make an effective comparison, the same curve for Type B pulse-forming network is also shown in figure 8. Analysis shows that the graphs for Type B and Type C pulse-forming networks are almost identical, as it is stated in the literature [4, 7]. It clearly indicates that the developed computer models are valid because they are precise and correctly explain all the processes taking place in the systems.

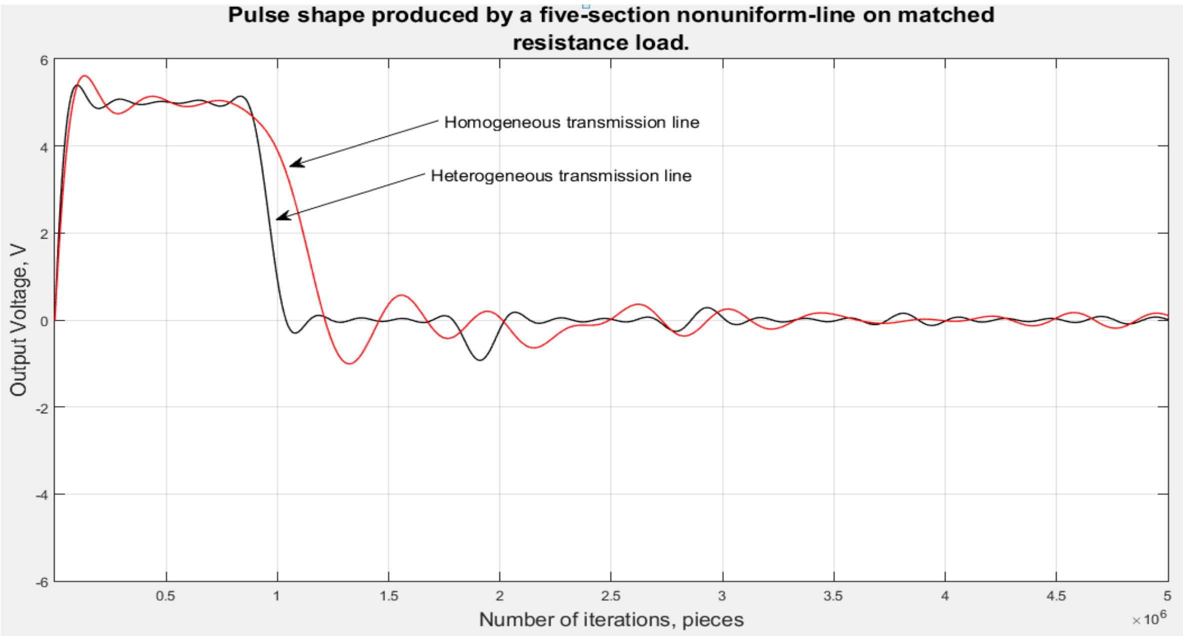

Figure 7: Pulse shape produced by heterogeneous Type B pulse-forming network with 5 elements on matched load

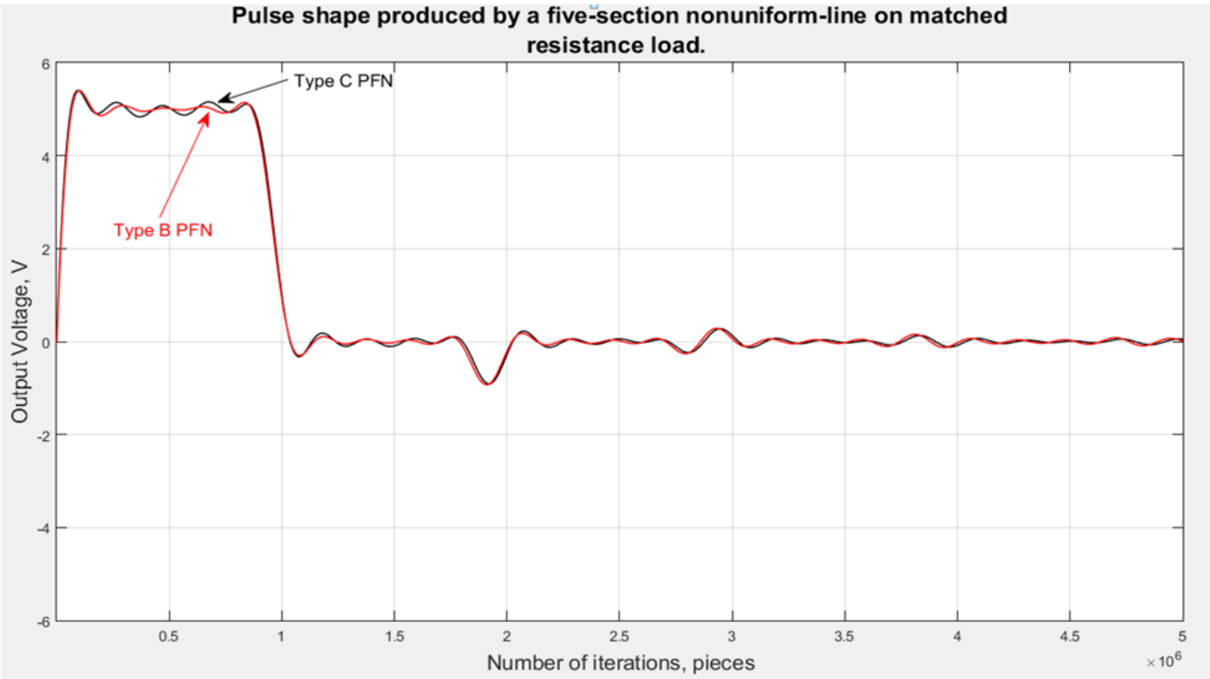

Figure 8: Pulse shape produced by heterogeneous Type C pulse-forming network with 5 elements on matched load

6. Conclusion

In this paper an alternative approach to studying transient processes in pulse-forming networks has been proposed. This approach, which is based on computer simulation in the Matlab environment, has been tested in different scenarios for two different artificial transmission lines. Simulation results proved its validity because those results comply with the general understanding of the processes in pulse-forming networks and support the conclusions and assumptions made in scientific literature by other authors. In addition, this approach is simple, clear and can be scaled down or up and modified to adjust to the purpose of a study. Designed computer models can be used in carrying out promising research in the field.

Table 2
Values of capacitors and inductors to form a trapezoidal pulse in Type C PFN

Stage number	Capacitor value	Inductance value
1	0.4003	0.253
2	0.0416	0.270
3	0.0111	0,367
4	0,0038	0.547
5	0.0017	0.740

7. References

[1] C. Wolff, Radar Modulator, 2021. URL: http:// www.radartutorial.eu/08.transmitters/Radar%20Modulator.en.html
[2] Handbook of RF and Microwave Power Amplifiers. Ed. J. Walker, Cambridge University Press, Cambridge UK, 2012.
[3] A. Eroglu, Introduction to RF Power Amplifier Design and Simulation. New York: CRC Press Taylor & Francis Group, 2016.
[4] Ness Engineering Inc., Pulse Forming Network Equations and Calculator, 2021, http://www.nessengr.com/technical-data/pulse-forming-network-pfn-equations-and-calculator/#TypeB
[5] L. E. Frenzel Jr., Principles of electronic communication systems, 4th ed., McGraw-Hill Education, New York, NY, 2016.
[6] W. McC. Siebert, Circuits, Signals, and Systems, Cambridge, McGraw-Hill Book Company, MA, 1986. https://doi.org/10.7551/mitpress/1839.001.0001.
[7] Pulse Generators, Ed. G. Glasoe. McGraw-Hill Book Company, NY, 1948.
[8] Radio Frequency and Microwave Power Amplifiers. Volume 1: Principles, Device Modeling and Matching Networks. Ed. A. Grebennikov. The Institution of Engineering and Technology, London, UK, 2019.
[9] Radio Frequency and Microwave Power Amplifiers. Volume 2: Efficiency and Linearity Enhancement Techniques. Ed. A. Grebennikov. The Institution of Engineering and Technology, London UK, 2019.
[10] M. K. Kazimierczuk, RF Power Amplifiers, Wiley, Chichester UK, 2008.
[11] O. Pliushch, S. Toliupa, A. Rybydajlo. "Studying Characteristics of Transmission Lines with Help of Computer Simulation in the Matlab Environment," presented at the IEEE International Scientific-Practical Conference PIC S&T, Kyiv, Ukraine, October 5–7, 2021, Paper 111, in press.
[12] O. Pliushch, "Gradient Signal Processing Algorithm for Adaptive Antenna Arrays Obviating Reference Signal Presence," presented at the IEEE International Scientific-Practical Conference PIC S&T, Kyiv, Ukraine, October 8–11, 2019, Paper 190. https://doi.org/10.1109/PICST47496.2019.9061536.
[13] O. Pliushch, V. Vyshnivskyi, S. Toliupa, A. Rybydajlo. "Utilization of Clipper Circuits to Improve Efficiency of the Gradient Signal Processing Algorithm for Adaptive Antenna Arrays" // Proceedings of the 2019 IEEE International Conference on Advanced Trends in Information Theory (IEEE ATIT 2019). Kyiv, Ukraine, December 18-20, 2019. Paper 71. https://doi.org/10.1109/ATIT49449.2019.9030529.
[14] Radar Handbook, 3rd ed., Ed. in Chief M. I. Skolnik, McGraw-Hill Companies, NY, 2008.
[15] D. K. Barton, Radar Equations for Modern Radar, Artech House, MA, 2013.
[16] S. Russell, P. Norvig, Artificial Intelligence, A Modern Approach, Prentice Hall, 2003.
[17] A. Sobchuk, Y. Kravchenko, Y. Tyshchenko, M. Gawliczek, O. Afanasyeva, Analytical aspects of providing a feature of the functional stability according to the choice of technology for construction of wireless sensor networks, in: Proceedings of IEEE International Conference on Advanced Trends in Information Theory, ATIT'2019, Kyiv, 2019, pp. 102-106. doi: 10.1109/ATIT49449.2019.9030474.
[18] E. Mizraji, Vector logics: The matrix-vector representation of logical calculus, Fuzzy Sets and Systems (1992) pp. 179–185. doi: 10.1016/0165-0114(92)90216-Q.
[19] J.F. Luger, Artificial Intelligence. Strategies and methods for solving complex problems, 2003.
[20] K.Park, K.Lee, S.Park, H.Lee, Telecommunication node clustering with node compatibility and network survivability requirements, Management Science, vol. 46(3), 2000, pp.363-374.